Coupling Characterization of a Linear Dipole Array to Improve Direction-of-Arrival Estimation

Kuan-Hao Chen and Jean-Fu Kiang

***Abstract*—The reciprocity theorem is applied to account for the electromagnetic coupling among antennas in a linear dipole array, in the presence of multiple incident plane waves. By utilizing the direction-dependent coupling information, the direction-of-arrivals of the incident waves can be estimated more accurately by using the conventional ESPRIT (estimation of signal parameter via rotational invariance technique). Different coupling compensation methods in the literatures are compared to validate this method, and multiple incident waves of both uncorrelated and coherent nature are also simulated.**

***Index Terms*—Direction of arrival estimation, linear antenna arrays, mutual coupling.**

I. Introduction

DIRECTION-OF-ARRIVAL (DOA) can be estimated by processing the receiving signals of the antenna arrays, with signal-processing algorithms like multiple signal classification (MUSIC), root-MUSIC, estimation of signal parameters via rotational invariance technique (ESPRIT) [1]–[4], matrix pencil method [5], and discrete Fourier transform-based method [6].

These algorithms may produce inaccurate DOA estimation if the electromagnetic coupling among antennas of the receiving array is not well accounted for. Different methods have been proposed to mitigate the mutual coupling effects [7]–[11]. A mutual coupling matrix is usually defined and computed to compensate for the coupling effects before applying signal-processing algorithms for beamforming or DOA estimation [12]–[13].

In [7], a mutual impedance was used to derive the open-circuit voltages by using the received voltages, which were then used to adjust certain parameters of adaptive arrays. This method was used in [12] to improve the accuracy of DOA estimation with a dipole array.

In [8], an improved compensation method was proposed to compensate for the coupling effects embedded in the received voltages, by using a full-wave approach. However, the incident angles must be known *a priori*.

Manuscript received August 05, 2014; revised July 14, 2015; accepted September 09, 2015. Date of publication September 14, 2015; date of current version October 28, 2015. This work was supported in part by the Ministry of Science and Technology, Taiwan, ROC, under Grant NSC 102-2221-E-002-043, and in part by the Ministry of Education, Taiwan, under Aim for Top University Project 103R3401-1.

The authors are with the Graduate Institute of Communication Engineering, National Taiwan University, Taipei 106, Taiwan (e-mail: jfkiang@ntu.edu.tw).

Digital Object Identifier 10.1109/TAP.2015.2478475

In [9], a minimum-norm mutual coupling compensation technique [3] was applied to process the array signals. Both the matrix pencil method [5] and the MUSIC [1] algorithm were also used for comparison.

In [10], a calibration method was proposed, in which the mutual coupling matrix is obtained by processing the receiving voltages with and without coupling, respectively. This method deals with data in the signal space, and does not need the electromagnetic response of the array.

In [11], a modified mutual impedance was proposed by including the open-circuit scattering effects and the load impedances in the receiving array. The accuracy of this method is better than that of the conventional open-circuit voltage method if followed by the MUSIC algorithm.

In this work, the reciprocity theorem is applied to model the mutual coupling effects in a linear dipole array, where the driving voltage sources and source impedances in the transmitting mode as well as the load impedances in the receiving mode are rigorously related to the impedance matrix, leading to more accurate DOA estimation with an ESPRIT algorithm. Simulation results are validated and compared with the literatures.

This paper is organized as follows. The signal model is presented in Section II, the conventional decoupling method is briefly reviewed in Section III, the proposed decoupling method is presented in Section IV, the covariance matrix needed for the ESPRIT is derived in Section V. Simulation results are presented and discussed in Section VI. Finally some conclusion is drawn in Section VII.

II. Signal Model

Fig. 1 shows linear array of N_d dipoles operating in the transmitting mode and the receiving mode, respectively. When there are M plane waves incident upon the array, the received voltages at all the antenna loads $\bar{V}_r = [v_{r1}, v_{r2}, \ldots, v_{rN_d}]^t$ can be expressed as

$$\begin{aligned}\bar{V}_r(t) &= \sum_{m=1}^{M} \bar{a}(\phi_m) s_m(t) + \bar{n}(t) \\ &= \bar{\bar{D}}(\phi) \cdot \bar{s}(t) + \bar{n}(t) \end{aligned} \tag{1}$$

where $\bar{a}(\phi_m)$ is an $N_d \times 1$ steering vector associated with the mth plane wave, which has the amplitude $s_m(t)$ and is incident from direction ϕ_m; $\bar{n}$ is an $N_d \times 1$ vector, recording noises at all the antenna loads; $\bar{\bar{D}}(\phi) = [\bar{a}(\phi_1) \ldots \bar{a}(\phi_M)]$ is an $N_d \times M$ matrix; and $\bar{s}(t) = [s_1(t) \ldots s_M(t)]^t$ is an $M \times 1$ vector.

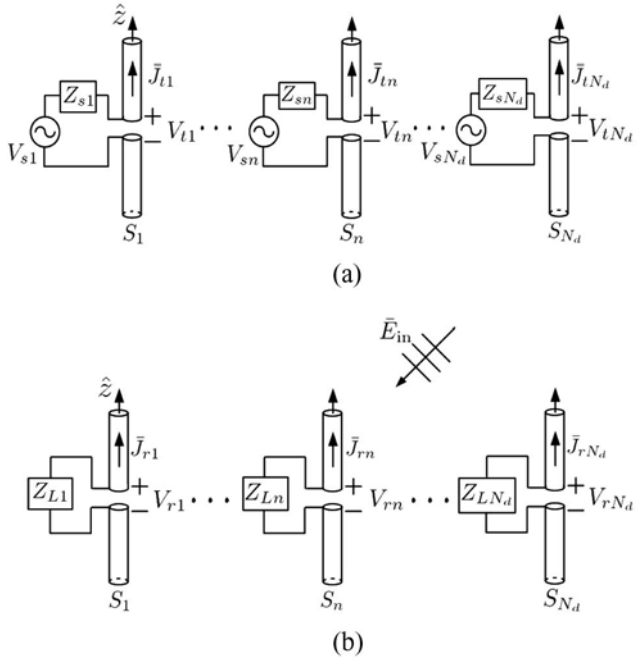

Fig. 1. Linear array of N_d dipoles. (a) Transmitting mode. (b) Receiving mode.

The coupling effects embedded in the received voltages $\bar{V}_r(t)$ are compensated via the mutual coupling matrix $\bar{\bar{C}}$ to obtain the decoupled voltages $\bar{V}$ as [7]–[11]

$$\bar{V}(t) = \bar{\bar{C}}^{-1} \cdot \bar{V}_r(t). \tag{2}$$

By substituting (1) into (2), we have

$$\bar{V}(t) = \bar{\bar{C}}^{-1} \cdot \bar{\bar{D}}(\phi) \cdot \bar{s}(t) + \bar{\bar{C}}^{-1} \cdot \bar{n}(t). \tag{3}$$

If the incident waves are uncorrelated to the noises, and the noises have identical variance of σ_n^2, the correlation matrix of $\bar{V}(t)$ can be expressed as

$$\begin{aligned}\bar{\bar{R}} &= \mathrm{E}\left\{\bar{V}(t)\bar{V}^{\dagger}(t)\right\} \\ &= \bar{\bar{C}}^{-1} \cdot \bar{\bar{D}} \cdot \bar{\bar{R}}_{ss} \cdot \bar{\bar{D}}^{\dagger} \cdot (\bar{\bar{C}}^{-1})^{\dagger} + \bar{\bar{C}}^{-1} \cdot \bar{\bar{R}}_{nn} \cdot (\bar{\bar{C}}^{-1})^{\dagger}.\end{aligned} \tag{4}$$

In numerical simulations, the correlation matrices are derived from K samples of data as

$$\begin{aligned}\bar{\bar{R}}_{ss} &\simeq \frac{1}{K}\sum_{k=1}^{K} \bar{s}[k]\bar{s}^{\dagger}[k] \\ \bar{\bar{R}}_{nn} &\simeq \frac{1}{K}\sum_{k=1}^{K} \bar{n}[k]\bar{n}^{\dagger}[k]\end{aligned} \tag{5}$$

where the Monte Carlo technique is applied to simulate $\bar{n}[k]$s. The covariance matrix is then input to conventional DOA estimation algorithms like ESPRIT to estimate the DOAs.

III. Conventional Decoupling Methods

A. Coupling Matrix Method

Method of moments has been applied to compute the receiving voltages of an N_d-dipole array as shown in Fig. 1(b), leading to a matrix equation [8]

$$\bar{V}_M = \bar{\bar{Z}} \cdot \bar{I} = \left(\bar{\bar{Z}}_M + \bar{\bar{Z}}_L\right) \cdot \bar{I} \tag{6}$$

which can be solved to have

$$\bar{I} = \bar{\bar{Z}}^{-1} \cdot \bar{V}_M = \bar{\bar{Y}} \cdot \bar{V}_M \tag{7}$$

where $\bar{\bar{Z}}_M$ is the impedance matrix, $\bar{\bar{Z}}_L$ is an $N_d \times N_d$ diagonal matrix, which contains all the load impedances, and $\bar{V}_M$ depends on the incident fields but is free of mutual coupling.

The receiving voltages, including the mutual coupling effects, can be expressed as [9]

$$\bar{V}_r = \bar{\bar{Z}}_L \cdot \bar{I}_P = \bar{\bar{Z}}_L \cdot \bar{\bar{Y}}_P \cdot \bar{V}_M \tag{8}$$

where $\bar{\bar{Y}}_P$ is an $N_d \times N_d Q$ submatrix of $\bar{\bar{Y}}_M$, Q is the number of basis functions implemented on each dipole. The elements of $\bar{V}_M$ can be expressed in terms of those at the antenna ports, thus (9) can be reduced to [8]

$$\bar{V}_r = \bar{\bar{C}} \cdot \bar{V}'_M \tag{9}$$

where $\bar{V}'_M$ contains N_d elements at the antenna ports, and $\bar{\bar{C}}$ is an $N_d \times N_d$ coupling matrix.

B. Calibration Method

The receiving-voltage vectors $\bar{V}_r$s, associated with different DOAs, are obtained and stored in a matrix as [10]

$$\bar{\bar{V}}_r = \left[\, \bar{V}_{r1} \;\; \bar{V}_{r2} \;\; \cdots \;\; \bar{V}_{rP} \,\right] \tag{10}$$

where $\bar{V}_{rp}$ is the receiving-voltage vector when a plane wave is incident in direction p, with $p = 1, 2, \ldots, P$. Typically, P is larger than N_d.

Consider a plane wave incident from the pth direction. The receiving voltage at each dipole of the array, in the absence of the other dipoles, is computed and stored in $\bar{V}_{dp}$. These vectors are then compiled into a matrix as

$$\bar{\bar{V}}_d = \left[\, \bar{V}_{d1} \;\; \bar{V}_{d2} \;\; \cdots \;\; \bar{V}_{dP} \,\right]. \tag{11}$$

A mutual coupling matrix $\bar{\bar{C}}$ is defined as

$$\bar{\bar{V}}_r = \bar{\bar{C}} \cdot \bar{\bar{V}}_d \tag{12}$$

from which the mutual coupling matrix can be estimated by using the least-square method as [10]

$$\bar{\bar{C}} = \bar{\bar{V}}_r \cdot \bar{\bar{V}}_d^{\dagger} \left(\bar{\bar{V}}_d \cdot \bar{\bar{V}}_d^{\dagger}\right)^{-1} \tag{13}$$

where $\bar{\bar{A}}^{\dagger}$ is the Hermitian of $\bar{\bar{A}}$.

C. Induced EMF Method

By applying the reciprocity theorem to the dipole array in the transmitting mode and the receiving mode, as shown in Fig. 1, the voltages and currents in these two modes are related as

$$\sum_{n=1}^{N_d}\left(V_{sn}-Z_{sn}I_{tn}\right)I_{rn}-\sum_{n=1}^{N_d}V_{rn}I_{tn} = -\bar{E}_{\text{in}}\cdot\sum_{n=1}^{N_d}\iint_{S_n}\bar{J}_{tn}(\bar{r}')e^{jk\hat{r}\cdot\bar{r}'}\,d\bar{r}' \tag{14}$$

where $V_{tn}=V_{sn}-Z_{sn}I_{tn}$, $I_{rn}=-V_{rn}/Z_{Ln}$, and $\hat{r}=\hat{x}\sin\theta_i\cos\phi_i+\hat{y}\sin\theta_i\sin\phi_i+\hat{z}\cos\theta_i$. By choosing $Z_{sn}=Z_{Ln}$ and $V_{sn}=\delta_{mn}$, the left-hand side of (15) can be reduced to $-(V_{sm}/Z_{Lm})V_{rm}$.

In the simulations, the incident waves are assumed to arrive in the horizontal directions, with the electric field $\bar{E}_{\text{in}}=-\hat{z}E_{\text{in}}$. The dipole radius is typically much smaller than one wavelength, hence the induced current is independent of the circumferential coordinate. Thus, the surface integrals in (15) can be reduced to

$$\iint_{S_n}\bar{J}_{tn}(\bar{r}')e^{jk\hat{r}\cdot\bar{r}'}\,d\bar{r}'=\int_{-L_n/2}^{L_n/2}\bar{I}_{tn}(z')e^{jk\hat{r}\cdot\bar{r}'}\,dz' \tag{15}$$

with $\bar{I}_{tn}(z')=2\pi a\bar{J}_{tn}(z')$.

Next, the transmitting current $\bar{J}_{tn}$ on the right-hand side of (15) is relabeled as

$$\bar{J}_{tn}(\bar{r}')=\begin{cases}\bar{J}_{t,mm}(\bar{r}'), & n=m\\ \bar{J}_{t,nm}(\bar{r}'), & n\neq m\end{cases} \tag{16}$$

where $\bar{J}_{t,mm}$ and $\bar{J}_{t,nm}$ are the transmitting current on the mth dipole and the induced current on the nth dipole, respectively. Then, (15) can be reduced to a matrix equation as

$$\bar{\bar{Z}}\cdot\bar{V}_r=-\bar{\bar{G}}\cdot\bar{E} \tag{17}$$

where

$$Z_{mn}=\begin{cases}\dfrac{V_{sm}}{Z_{Lm}I_{t,mm}(0)}, & m=n\\ 0, & m\neq n\end{cases}$$

$$G_{mn}=\begin{cases}\dfrac{1}{I_{t,mm}(0)}\displaystyle\int_{-L_m/2}^{L_m/2}I_{t,mm}(z')e^{jkz'\cos\theta_i}dz', & m=n\\ \dfrac{1}{I_{t,mm}(0)}\displaystyle\int_{-L_n/2}^{L_n/2}I_{t,nm}(z')e^{jkz'\cos\theta_i}dz', & m\neq n\end{cases}$$

$$E_n=E_0e^{jk\left(x'_n\sin\theta_i\cos\phi_i+y'_n\sin\theta_i\sin\phi_i\right)} \tag{18}$$

with $1\le m,n\le N_d$. Equation (18) implies that

$$\bar{V}_r=\bar{\bar{C}}\cdot\bar{E} \tag{19}$$

where $\bar{\bar{C}}=-\bar{\bar{Z}}^{-1}\cdot\bar{\bar{G}}$ is called the coupling matrix [14].

Note that the coupling matrices in (10), (14), and (20) share similar idea, but they are computed with different methods and carry different information.

IV. Decoupling Method With Azimuth Information

The current distribution on the mth dipole $\bar{I}_{t,mm}$ can be further decomposed into

$$\bar{I}_{t,mm}(\bar{r}')=\bar{I}_t(\bar{r}')+\bar{I}_{t,mc}(\bar{r}') \tag{20}$$

where $\bar{I}_t(\bar{r}')$ is the current distribution on a single dipole in the absence of the other dipoles, and

$$\bar{I}_{t,mc}(\bar{r}')=\sum_{n=1,n\neq m}^{N_d}\bar{I}_{t,mn}(\bar{r}') \tag{21}$$

is the current coupled from the other dipoles. Thus, (15) can be rewritten as

$$\bar{\bar{Z}}\cdot\bar{V}_r(\theta_i,\phi_i)+\bar{\bar{G}}'(\theta_i)\cdot\bar{E}(\theta_i,\phi_i)=\bar{\bar{A}}\cdot\bar{V}_{\text{oc}}(\theta_i,\phi_i) \tag{22}$$

where

$$G'_{mn}(\theta_i)=\begin{cases}\dfrac{1}{I_{t,mm}(0)}\displaystyle\int_{-L_m/2}^{L_m/2}I_{t,mc}(z')e^{jkz'\cos\theta_i}dz', & m=n\\ \dfrac{1}{I_{t,mm}(0)}\displaystyle\int_{-L_n/2}^{L_n/2}I_{t,nm}(z')e^{jkz'\cos\theta_i}dz', & m\neq n\end{cases}$$

$$A_{mn}=\begin{cases}I_t(0)/I_{t,mm}(0), & m=n\\ 0, & m\neq n\end{cases}$$

$$V_{\text{oc}m}(\theta_i,\phi_i)=-\frac{1}{I_t(0)}E_0e^{jk\left(x'_m\sin\theta_i\cos\phi_i+y'_m\sin\theta_i\sin\phi_i\right)}\int_{-L_m/2}^{L_m/2}dz'I_t(z')e^{jkz'\cos\theta_i}. \tag{23}$$

Equation (23) implies that

$$\bar{V}_{\text{oc}}(\theta_i,\phi_i)=\bar{\bar{A}}^{-1}\cdot\bar{\bar{Z}}\cdot\bar{V}_r(\theta_i,\phi_i)+\bar{\bar{A}}^{-1}\cdot\bar{V}_c(\theta_i,\phi_i) \tag{24}$$

where $\bar{V}_c(\theta_i,\phi_i)=\bar{\bar{G}}'(\theta_i)\cdot\bar{E}(\theta_i,\phi_i)$ is regarded as the coupling voltages from all other dipoles, which is a function of the incident direction. By choosing $\bar{V}_c$ with arguments close to the incident direction (θ_i,ϕ_i), the coupling effects can be better accounted for with (25).

V. Covariance Matrix for ESPRIT

The conventional ESPRIT algorithm will be used to estimate the DOAs of single or multiple incident plane waves. First, (25) is sampled at the kth time instant to have

$$\bar{V}_{\text{oc}}[k]=\bar{\bar{A}}^{-1}\cdot\bar{\bar{Z}}\cdot\bar{V}_r[k]+\bar{\bar{A}}^{-1}\cdot\bar{V}_c=\bar{\bar{B}}\cdot\left(\bar{V}_s[k]+\bar{n}[k]\right)+\bar{C} \tag{25}$$

with $\bar{\bar{B}}=\bar{\bar{A}}^{-1}\cdot\bar{\bar{Z}}$, $\bar{V}_r[k]=\bar{V}_s[k]+\bar{n}[k]$, and

$$\bar{C}=\sum_{m=1}^{M}\bar{C}_m=\sum_{m=1}^{M}A_m\bar{\bar{A}}^{-1}\cdot\bar{V}_c(\phi_m) \tag{26}$$

where A_m is the amplitude of the mth incident wave, assuming there are M incident waves.

Define a cost function

$$J = \left| \bar{V}_r' - \sum_{m=1}^{M} A_m \bar{V}_{\text{cal}}(\tilde{\phi}_m) \right|^2 \tag{27}$$

where $\bar{V}_r'$ is the average of $\bar{V}_r[k]$'s over K samples, and $\bar{V}_{\text{cal}}(\tilde{\phi}_m)$ contains the receiving voltages when a plane wave with unit-amplitude is incident at $\tilde{\phi}_m$. By setting $\partial J/\partial A_m^* = 0$, a matrix equation is derived as

$$\sum_{m=1}^{M} \bar{V}_{\text{cal}}^{\dagger}(\tilde{\phi}_{m'}) \cdot \bar{V}_{\text{cal}}(\tilde{\phi}_m) A_m = \bar{V}_{\text{cal}}^{\dagger}(\tilde{\phi}_{m'}) \cdot \bar{V}_r' \tag{28}$$

with $1 \le m' \le M$ from which the amplitudes A_ms can be determined. The initial guess of $\tilde{\phi}_m$s can be obtained by applying the ESPRIT algorithm to a conventional covariance matrix like that in (5).

Assume that the signals and the noises are uncorrelated, and the noises have zero mean, namely, $\mathrm{E}\{\bar{V}_s \bar{n}^{\dagger}\} = \mathrm{E}\{\bar{n}\bar{V}_s^{\dagger}\} = 0$ and $\mathrm{E}\{\bar{n}\} = 0$. Then, the covariance matrix of $\bar{V}_{\text{oc}}$ can be derived as

$$\begin{aligned} \bar{\bar{R}} = \mathrm{E}\{\bar{V}_{\text{oc}} \bar{V}_{\text{oc}}^{\dagger}\} &= \bar{\bar{B}} \cdot \bar{\bar{R}}_{ss} \cdot \bar{\bar{B}}^{\dagger} + \bar{\bar{B}} \cdot \bar{X}_s \bar{C}^{\dagger} \\ &+ \bar{\bar{B}} \cdot \bar{\bar{R}}_{nn} \cdot \bar{\bar{B}}^{\dagger} + \bar{C}\bar{X}_s^{\dagger} \cdot \bar{\bar{B}}^{\dagger} + \bar{C}\bar{C}^{\dagger} \end{aligned} \tag{29}$$

where

$$\begin{aligned} \bar{\bar{R}}_{ss} &= \mathrm{E}\{\bar{V}_s \bar{V}_s^{\dagger}\} \simeq \frac{1}{K} \sum_{k=1}^{K} \bar{V}_s[k] \bar{V}_s^{\dagger}[k] \\ \bar{\bar{R}}_{nn} &= \mathrm{E}\{\bar{n}\bar{n}^{\dagger}\} \simeq \frac{1}{K} \sum_{k=1}^{K} \bar{n}[k] \bar{n}^{\dagger}[k] \\ \bar{X}_s &= \mathrm{E}\{\bar{V}_s\} \simeq \frac{1}{K} \sum_{k=1}^{K} \bar{V}_s[k]. \end{aligned} \tag{30}$$

If the M incident waves are uncorrelated to one another, (30) can be reduced to

$$\begin{aligned} \bar{\bar{R}} = \bar{\bar{B}} \cdot \bar{\bar{R}}_{ss} \cdot \bar{\bar{B}}^{\dagger} &+ \sum_{m=1}^{M} \bar{\bar{B}} \cdot \bar{X}_{sm} \bar{C}_m^{\dagger} + \bar{\bar{B}} \cdot \bar{\bar{R}}_{nn} \cdot \bar{\bar{B}}^{\dagger} \\ &+ \sum_{m=1}^{M} \bar{C}_m \bar{X}_{sm}^{\dagger} \cdot \bar{\bar{B}}^{\dagger} + \sum_{m=1}^{M} \bar{C}_m \bar{C}_m^{\dagger} \end{aligned} \tag{31}$$

with

$$\bar{X}_{sm} = \mathrm{E}\{\bar{V}_{sm}\} \simeq \frac{1}{K} \sum_{k=1}^{K} \bar{V}_{sm}[k] \tag{32}$$

where $\bar{V}_{sm}$ contains the received voltages induced by the mth incident wave.

The covariance matrix $\bar{\bar{R}}$ is then processed with the ESPRIT algorithm to get a more accurate estimation of ϕ'', with the initial guess ϕ' obtained by using the conventional methods.

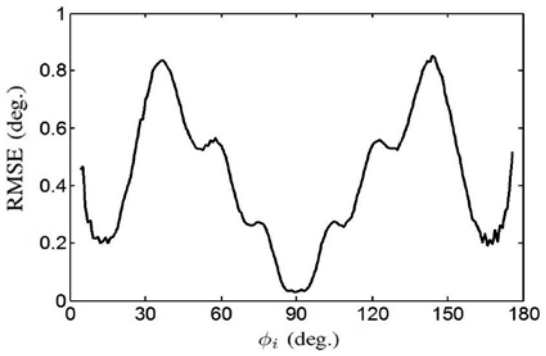

Fig. 2. RMSE of DOA over 100 Monte Carlo realizations, without compensating the mutual coupling, $K = 300$, $N_d = 7$, and SNR $= 3$ dB.

VI. Results and Discussions

Consider a linear dipole array with $N_d = 7$, deployed along the x-axis at a uniform spacing of $d = \lambda/2$ at 2.4 GHz. All the dipoles are polarized in the z direction, have the length $L = \lambda/2$ and radius $a = \lambda/200$. The amplitude of the incident waves is $A = 15$ (mV/m).

The noise can be specified in terms of the signal-to-noise ratio (SNR) as

$$\text{SNR} = \frac{\mathrm{E}\{\bar{V}_s^{\dagger} \cdot \bar{V}_s\}}{\mathrm{E}\{\bar{n}^{\dagger} \cdot \bar{n}\}} = \frac{\mathrm{E}\{\bar{V}_s^{\dagger} \cdot \bar{V}_s\}}{N_d \sigma_n^2} \tag{33}$$

where $n_\ell = n_\ell' + j n_\ell''$ with $1 \le \ell \le N_d$. Both n_ℓ' and n_ℓ'' are real Gaussian random variables with variance $\sigma_n^2/2$.

The accuracy of DOA estimation is evaluated in terms of the root-mean-squared error (RMSE) over N realizations of Monte Carlo simulations as

$$\text{RMSE} = \sqrt{\frac{1}{N} \sum_{n=1}^{N} \sum_{m=1}^{M} \left(\phi_{n,m}'' - \phi_{n,m}\right)^2} \tag{34}$$

where $\phi_{n,m}$ and $\phi_{n,m}''$ are the true DOA and the estimated DOA, respectively, of the mth incident angle in the nth realization.

Fig. 2 shows the RMSE of DOA over 100 Monte Carlo realizations, without compensating the mutual coupling. The estimated DOA can be used as the initial guess ϕ_r, around which the proposed method can be applied over a relatively finer angular region to acquire a more accurate DOA estimation.

Next, we apply the ESPRIT algorithm to estimate the DOA by using the decoupled voltages derived from (25), the coupling matrix method [8] and the calibration method [10], respectively. The accuracy achieved with each method is evaluated over 100 Monte Carlo realizations.

Fig. 3 shows the effect of SNR on RMSE by using the proposed method for coupling compensation before applying the ESPRIT. For comparison, Fig. 4 shows the counterparts by using the coupling matrix or calibration method before applying the ESPRIT. The RMSE by using the proposed method is 0.0427° and 0.0941° at the DOA of 60° and 30°, respectively, at SNR $= 3$ dB; which are better than the corresponding RMSE of 0.1187° and 0.2711°, respectively, by using the other methods.

Fig. 5 shows the RMSE at different DOAs by using different coupling compensation methods. It is observed that the

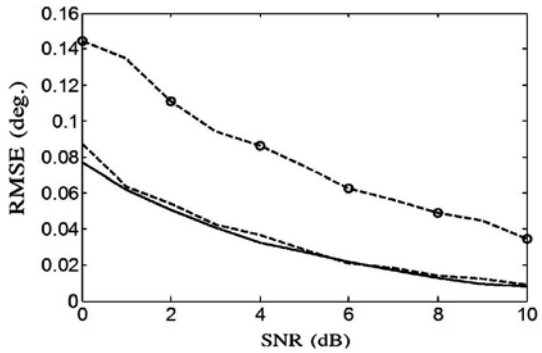

Fig. 3. Effect of SNR on RMSE by using the proposed method, with DOA at $\phi = 90^\circ$ (———), $\phi = 60^\circ$ ($- - -$), and $\phi = 30^\circ$ ($- \circ -$); over 100 Monte Carlo realizations, $K = 300$, $N_d = 7$.

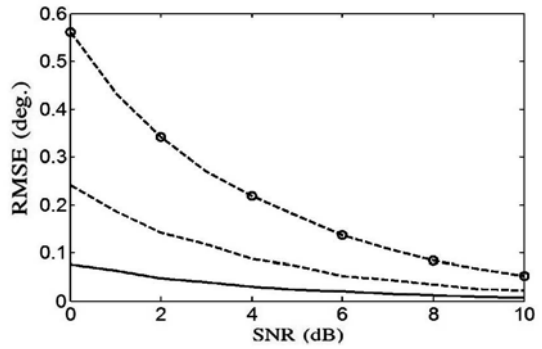

Fig. 4. Effect of SNR on RMSE by using the coupling matrix or calibration method, with DOA at $\phi = 90^\circ$ (———), $\phi = 60^\circ$ ($- - -$), and $\phi = 30^\circ$ ($- \circ -$); over 100 Monte Carlo realizations, $K = 300$, $N_d = 7$.

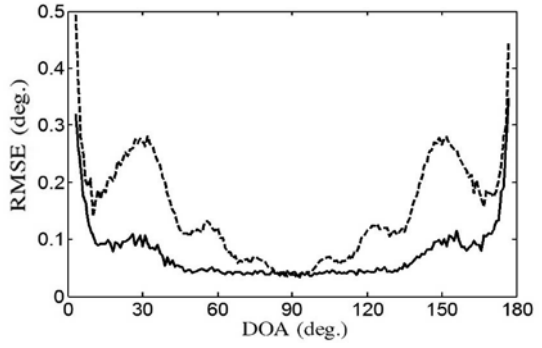

Fig. 5. RMSE at different DOAs by using the proposed method (———), coupling matrix or calibration method ($- - -$); over 100 Monte Carlo realizations, $K = 300$, $N_d = 7$, and SNR $= 3$ dB.

proposed method estimates the DOA more accurately than the other two methods.

Next, we will try to estimate the DOAs when there are multiple incident waves. Note that the source covariance matrix $\bar{\bar{R}}_{ss}$ in (5) is a diagonal matrix if the incident waves are uncorrelated, a nondiagonal and nonsingular matrix if the incident waves are partially correlated, and a nondiagonal but singular matrix if some incident waves are fully correlated [15]. Multipath signals originated from the same signal source will make the received signals highly correlated. In such cases, both

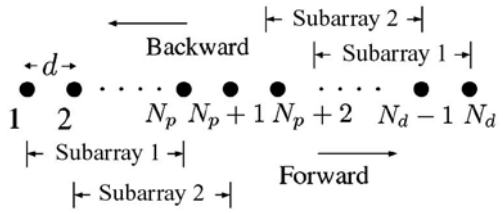

Fig. 6. Spatial smoothing technique with overlapping subarrays.

MUSIC and ESPRIT algorithms will fail because the source covariance matrix $\bar{\bar{R}}_{ss}$ becomes rank deficient.

The spatial smoothing technique [15] and forward/backward spatial smoothing (FBSS) technique [16] have been proposed to deal with such cases. By applying the FBSS technique, a modified covariance matrix is derived as

$$\bar{\bar{R}}_{fb} = \frac{1}{2}\left(\bar{\bar{R}}_f + \bar{\bar{R}}_b\right) \tag{35}$$

where $\bar{\bar{R}}_f$ and $\bar{\bar{R}}_b$ are the forward and backward spatially smoothed covariance matrices, respectively. It works as if the original array is grouped into multiple overlapping subarrays, and the average of the covariance matrices of all the subarrays is utilized to recover the rank of the source covariance matrix $\bar{\bar{R}}_{ss}$ before applying the ESPRIT algorithm.

Fig. 6 shows a uniform linear array of N_d dipoles, grouped into overlapping subarrays, each having N_p adjacent dipoles. The subarrays are labeled in both the forward and the backward directions, respectively. For example, dipoles $1, \ldots, N_p$ are grouped into the first forward subarray, dipoles $2, \ldots, N_p + 1$ into the second forward subarray, and so on. Let $\bar{U}_{f,q}[k]$ contain the open-circuit voltages of dipoles in the qth forward subarray. The forward spatially smoothing covariance matrix is calculated as the sample mean of the subarray covariance matrices as

$$\bar{\bar{R}}_f = \frac{1}{KP}\sum_{k=1}^{K}\sum_{q=1}^{P}\bar{U}_{f,q}[k]\bar{U}_{f,q}^{\dagger}[k] \tag{36}$$

where $P = N_d - N_p + 1$ is the number of subarrays, with $P \geq M$ and $N_p \geq M + 1$ [15].

Similarly, let $\bar{U}_{b,q}[k]$ contain the open-circuit voltages of dipoles in the qth backward subarray. The backward spatially smoothing covariance matrix is calculated as

$$\bar{\bar{R}}_b = \frac{1}{KP}\sum_{k=1}^{K}\sum_{q=1}^{P}\bar{U}_{b,q}^{*}[k]\left(\bar{U}_{b,q}^{*}[k]\right)^{\dagger} \tag{37}$$

where the superscript $*$ indicates complex conjugate. The matrices $\bar{\bar{R}}_f$ and $\bar{\bar{R}}_b$ are substituted into (36) to derive $\bar{\bar{R}}_{fb}$, which is then used in the ESPRIT algorithm.

Fig. 7 shows the effect of SNR on RMSE, under two uncorrelated incident waves. Since the proposed method is capable of eliminating the mutual coupling more effectively than the other two methods, hence the RMSE of the former is lower than that of the latter, especially at lower SNRs. For example, the difference of RMSE is about 0.3° at SNR $= 3$ dB.

Fig. 8 shows the effect of SNR on RMSE, under two correlated incident waves. The FBSS technique is applied to recover

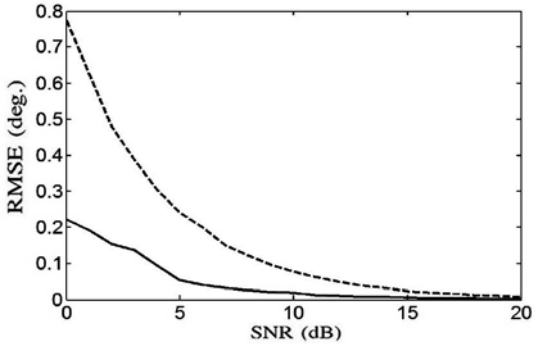

Fig. 7. Effect of SNR on RMSE, under two uncorrelated waves incident from $\phi_1 = 30^\circ$ and $\phi_2 = 60^\circ$, respectively; ———: with the proposed method, $- - -$: with coupling matrix or calibration method; over 100 Monte Carlo realizations, $K = 300$, $N_d = 7$.

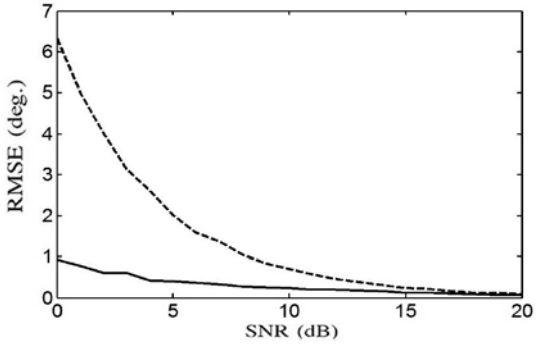

Fig. 8. Effect of SNR on RMSE, under two correlated waves incident from $\phi_1 = 30^\circ$ and $\phi_2 = 60^\circ$, respectively; ———: with the proposed method, $- - -$: with coupling matrix or calibration method; over 100 Monte Carlo realizations, $K = 300$, $N_p = 5$, and $N_d = 7$.

the rank deficiency of $\bar{\bar{R}}_{ss}$ due to correlation of the incident waves. The size of each subarray is set to $N_p = 5$, and $\bar{\bar{R}}_f$ and $\bar{\bar{R}}_b$ are derived from the decoupled voltages.

Compared to Fig. 7, the RMSE under two correlated incident waves is generally higher than that with two uncorrelated ones because stronger coupling among dipoles is induced in the former case than in the latter. Since the proposed method takes the azimuth information into account, it is more accurate than the other two methods.

Fig. 9 shows the RMSE under two uncorrelated incident waves, where ϕ_1 is varied from 85° to 5° while ϕ_2 is fixed at 90°. It is observed that the RMSE with the proposed method is lower than that with the other two methods, especially when the difference of incident angles between these two waves is close to 5°.

Fig. 10 shows the RMSE, under two correlated incident waves, where ϕ_1 is varied from 75° to 5° while ϕ_2 is fixed at 90°. At SNR = 10 dB, two correlated waves with incident angles as close as 15° can be resolved with the proposed method, and two uncorrelated waves with incident angles separated by 5° can also be resolved. If the incident angles of the two correlated waves become small or if the SNR is low, the DOA estimation algorithm will misjudge these two waves as one, leading to a higher RMSE. In short, to enhance the DOA resolution demands a higher SNR or a larger array.

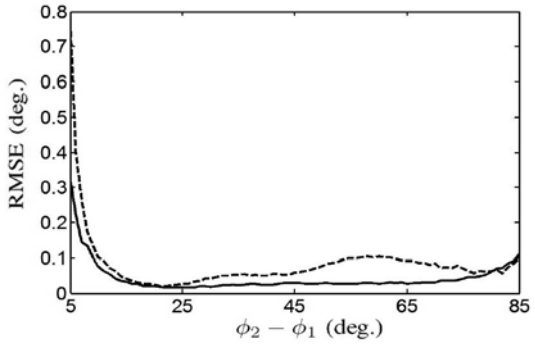

Fig. 9. RMSE under two uncorrelated waves incident from $85^\circ \geq \phi_1 \geq 5^\circ$ and $\phi_2 = 90^\circ$, respectively; ———: with the proposed method, $- - -$: with coupling matrix or calibration method; over 100 Monte Carlo realizations, $K = 300$, SNR = 10 dB, and $N_d = 7$.

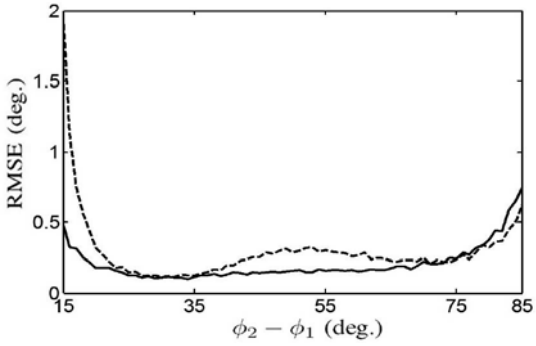

Fig. 10. RMSE under two correlated waves incident from $75^\circ \geq \phi_1 \geq 5^\circ$ and $\phi_2 = 90^\circ$, respectively; ———: with the proposed method, $- - -$: with coupling matrix or calibration method; over 100 Monte Carlo realizations, $K = 300$, SNR = 10 dB, $N_p = 5$, and $N_d = 7$.

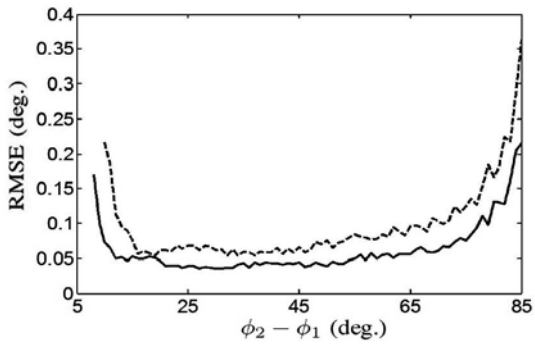

Fig. 11. RMSE under two correlated incident waves with the proposed method, $\phi_2 = 90^\circ$; ———: $82^\circ \geq \phi_1 \geq 5^\circ$, $N_d = 15$; $- - -$: $80^\circ \geq \phi_1 \geq 5^\circ$, $N_d = 11$; over 100 Monte Carlo realizations, $K = 300$, SNR = 10 dB, and $N_p = 5$.

Fig. 11 shows the effect of array size (N_d) on the RMSE, under two correlated incident waves. It is observed that the DOA resolution is about 8° when $N_d = 15$, and is about 10° when $N_d = 11$, at SNR = 10 dB. The RMSE grows gradually as $\phi_1 < 15^\circ$, which means that the ESPRIT algorithm becomes less accurate when one of the waves is incident near the end-fire direction of the linear array.

VII. Conclusion

A coupling compensation method, which is derived by using the reciprocity theorem, has been proposed to decouple the receiving voltages on a linear dipole array. By applying the ESPRIT algorithm to these decoupled voltages, the DOAs of incident waves can be estimated more accurately than using the conventional coupling matrix or calibration methods. Multiple incident waves of uncorrelated or correlated nature have been simulated. The results indicate that the proposed method enhances the accuracy and resolution of DOAs obtained with the conventional methods.

References

[1] R. O. Schmidt, "Multiple emitter location and signal parameter estimation," *IEEE Trans. Antennas Propag.*, vol. 34, no. 3, pp. 276–280, Mar. 1986.

[2] R. Roy and T. Kailath, "ESPRIT—Estimation of signal parameters via rotational invariance techniques," *IEEE Trans. Acoust. Speech Signal Process.*, vol. 37, no. 7, pp. 984–995, Jul. 1989.

[3] F. Gross, *Smart Antennas for Wireless Communications*. New York, NY, USA: McGraw-Hill, 2005.

[4] L. C. Godara, "Application of antenna arrays to mobile communications. II. Beam-forming and direction-of-arrival considerations," *Proc. IEEE*, vol. 85, no. 8, pp. 1195–1245, Aug. 1997.

[5] Y. Hua and T. K. Sarkar, "Matrix pencil method for estimating parameters for exponentially damped/undamped sinusoids in noise," *IEEE Trans. Acoust. Speech Signal Process.*, vol. 38, no. 5, pp. 814–824, May 1990.

[6] T. Sarkar, M. Wicks, M. Salazar-Palma, and R. Bonneau, *Smart Antenna*. Hoboken, NJ, USA: Wiley/IEEE Press, 2003.

[7] I. J. Gupta and A. A. Ksienski, "Effect of mutual coupling on the performance of adaptive arrays," *IEEE Trans. Antennas Propag.*, vol. 31, no. 5, pp. 785–791, Sep. 1983.

[8] R. S. Adve and T. K. Sarkar, "Compensation for the effects of mutual coupling on direct data domain adaptive algorithms," *IEEE Trans. Antennas Propag.*, vol. 48, no. 1, pp. 86–94, Jun. 2000.

[9] C. K. E. Lau, R. S. Adve, and T. K. Sarkar, "Minimum norm mutual coupling compensation with applications in direction of arrival estimation," *IEEE Trans. Antennas Propag.*, vol. 52, no. 8, pp. 2034–2041, Aug. 2004.

[10] K. R. Dandekar, H. Ling, and G. Xu, "Experimental study of mutual coupling compensation in smart antenna applications," *IEEE Trans. Wireless Commun.*, vol. 1, no. 3, pp. 480–487, Jul. 2002.

[11] H. T. Hui, "Improved compensation for the mutual coupling effect in a dipole array for direction finding," *IEEE Trans. Antennas Propag.*, vol. 51, no. 9, pp. 2498–2503, Sep. 2003.

[12] C. C. Yeh, M. L. Leou, and D. R. Ucci, "Bearing estimations with mutual coupling present," *IEEE Trans. Antennas Propag.*, vol. 37, no. 10, pp. 1332–1335, Oct. 1989.

[13] H. T. Hui, "A practical approach to compensate for the mutual coupling effect in an adaptive dipole array," *IEEE Trans. Antennas Propag.*, vol. 52, no. 5, pp. 1262–1269, May 2004.

[14] S. Henault, Y. M. M. Antar, S. Rajan, R. Inkol, and S. Wang, "The multiple antenna induced EMF method for the precise calculation of the coupling matrix in a receiving antenna array," *Progr. Electromagn. Res. M*, vol. 8, pp. 103–118, 2009.

[15] T. J. Shan, M. Wax, and T. Kailath, "On spatial smoothing for direction-of-arrival estimation of coherent signals," *IEEE Trans. Acoust. Speech Signal Process.*, vol. 33, no. 4, pp. 806–811, Aug. 1985.

[16] S. U. Pillai and B. H. Kwon, "Forward/backward spatial smoothing techniques for coherent signal identification," *IEEE Trans. Acoust. Speech Signal Process.*, vol. 7, no. 1, pp. 8–15, Jan. 1989.

Kuan-Hao Chen was born in Tainan, Taiwan. He received the B.S. degree in electrical engineering from the National University of Tainan, Tainan, Taiwan, and the M.S. degree from the Graduate Institute of Communication Engineering, National Taiwan University, Taipei, Taiwan, in 2012 and 2014, respectively.

His research interests include mutual coupling compensation methods in various smart antenna arrays and MIMO antenna systems.

Jean-Fu Kiang received the Ph.D. degree in electrical engineering from the Massachusetts Institute of Technology, Cambridge, MA, USA, in 1989.

Since 1999, he has been a Professor with the Department of Electrical Engineering, Graduate Institute of Communication Engineering, National Taiwan University, Taipei, Taiwan. His research interests include electromagnetic applications, including antennas and arrays, wave propagation in ionosphere and atmosphere, satellite navigation, remote sensing and microwave systems.